OFFICE OF NAVAL RESEARCH

CONTRACT NO. N00014-86-K-0772

TECHNICAL REPORT NO. 9

Light Extinction in a Dispersion of Small Nematic Droplets

by

S. Zumer, A. Golemme, and J. W. Doane

Liquid Crystal Institute*
Kent State University
Kent, OH 44242

*Subcontractor to
Liquid Crystalline Polymer Research Center
University of Connecticut
Storrs, CT 06268

Prepared for Publication

in

Journal of Optical Society of America

July 13, 1988

AD-A197 201

-88

Unclassified
Security Classification of this page

REPORT DOCUMENTATION PAGE

1a. REPORT SECURITY CLASSIFICATION		1b. RESTRICTIVE MARKINGS			
Unclassified		None			
2a. SECURITY CLASSIFICATION AUTHORITY		3. DISTRIBUTION/AVAILABILITY OF REPORT			
		Approved for Public Release, Distribution Unlimited			
2b. DECLASSIFICATION/DOWNGRADING SCHEDULE					
4. PERFORMING ORGANIZATION REPORT NUMBER(S)		5. MONITORING ORGANIZATION REPORT NUMBER(S)			
Technical Report No. 9					
6a. NAME OF PERFORMING ORGANIZATION	6b. OFFICE SYMBOL (If applicable)	7a. NAME OF MONITORING ORGANIZATION			
University of Connecticut		Office of Naval Research			
6c. ADDRESS (City, State, and ZIP Code)		7b. ADDRESS (City, State, and ZIP Code)			
Storrs, CT 06268		800 North Quincy Avenue Arlington, VA 22217			
8a. NAME OF FUNDING/SPONSORING ORGANIZATION	8b. OFFICE SYMBOL (If applicable) ONR	9. PROCUREMENT INSTRUMENT IDENTIFICATION NUMBER			
		N00014-86-K-0772			
8c. ADDRESS (City, State, and ZIP Code)		10. SOURCE OF FUNDING NUMBERS			
800 North Quincy Avenue Arlington, VA 22217		PROGRAM ELEMENT NO	PROJECT NO	TASK NO	WORK UNIT ACCESSION NO

11. TITLE (Include Security Classification)
Light Extinction in a Dispersion of Small Nematic Droplets (Unclassified)

12. PERSONAL AUTHOR(S)
S. Zumer, A. Golemme, and J. W. Doane

13a. TYPE OF REPORT	13b. TIME COVERED	14. DATE OF REPORT (Year, Month, Day)	15. PAGE COUNT
Technical, Interim	FROM _____ TO 07/11/88	1988-07-11	43

17	COSATI CODES		18. SUBJECT TERMS (Continue on reverse if necessary and identify by block number)
FIELD	GROUP	SUB GROUP	Nematic droplets, Liquid Crystalline Polymers, Light Transmission properties, Rayleigh-Gans approximation.

19. ABSTRACT (Continue on reverse if necessary and identify by block number)

The light transmission properties of materials in which submicron size nematic droplets are dispersed in a solid polymeric matrix are studied. Theoretical calculations of the differential and total cross sections have been performed in the Rayleigh-Gans approximation for different nematic director configurations. The effect of interdroplet interference is discussed in relation to the droplet distribution, and different models for the pair correlation function are taken into account. An attenuation coefficient is defined and calculated for different director configurations. Theoretical calculations are in excellent agreement with experimental data obtained from thin films of materials consisting of droplets of cyanobiphenyls dispersed in an epoxy resin.

20. DISTRIBUTION/AVAILABILITY OF ABSTRACT	21. ABSTRACT SECURITY CLASSIFICATION
☒ UNCLASSIFIED/UNLIMITED ☐ SAME AS RPT ☐ DTIC USERS	Unclassified
22a. NAME OF RESPONSIBLE INDIVIDUAL	22b. TELEPHONE (Include Area Code) / 22c. OFFICE SYMBOL
Dr. Kenneth J. Wynne	(202) 696-4410 / ONR

DD FORM 1473, 84 MAR   83 APR edition may be used until exhausted.   SECURITY CLASSIFICATION OF THIS PAGE
All other editions are obsolete   Unclassified

LIGHT EXTINCTION IN A DISPERSION OF SMALL NEMATIC DROPLETS

S. Žumer,[1] A. Golemme,[2] and J.W. Doane

Liquid Crystal Institute

Kent State University

Kent, OH 44242

ABSTRACT

The light transmission properties of materials in which submicron size nematic droplets are dispersed in a solid polymeric matrix are studied. Theoretical calculations of the differential and total cross sections have been performed in the Rayleigh-Gans approximation for different nematic director configurations. The effect of interdroplet interference is discussed in relation to the droplet distribution, and different models for the pair correlation function are taken into account. An attenuation coefficient is defined and calculated for different director configurations. Theoretical calculations are in excellent agreement with experimental data obtained from thin films of materials consisting of droplets of cyanobiphenyls dispersed in an epoxy resin.

DTIC
COPY
INSPECTED
6

[1] Permanent address: Physics Department, E. Kardelj University of Ljubljana, 61000 Ljubljana, Yugoslavia.

[2] Permanent address: Department of Chemistry, University of Calabria, 87030 Rende (CS), Italy.

Accession For

NTIS   CR&I

Distribution/

Availability Codes

Dist	Avail and/or Special
A-1	

I . INTRODUCTION

Light extinction[1] in a random dispersion of small non-absorbing objects depends on their scattering properties and their distribution in space. Light scattering from a single object is a classical electromagnetic problem.[1-3] Exact solutions are known for few objects,[4,5] so that one is forced to use approximate approaches.[1] The most known simple approaches are: Rayleigh-Gans approximation[6,7] (RGA) for optically soft small objects, anomalous diffraction[1] (ADA) for large optically soft objects, and geometrical optics[1] for very large objects. In relative few studies optical anisotropy was taken into account.[2,8-11] The spatial distribution of the scattering objects influences the light extinction via two effects: the first one is interference[12,13] which predominently affects the distribution of the scattered light and to a lesser degree the total scattering cross section. The second effect is multiple scattering,[14] which is important when the path of light in the dispersion is long enough that the contribution of the indirect (scattered) light in the direction of the incident beam becomes substantial.

In the following we are going to study light extinction in materials consisting of a random dispersion of micron size nematic liquid crystal droplets in a polymeric matrix. These materials have been recently developed for use in optical and electrooptical devices.[11,15,16] Nematic droplets in a polymer are optically soft but anisotropic scattering objects. In most cases their indices of refraction $n_e \sim 1.7$ and $n_o \sim 1.5$ are close to the index of polymer $n_m \sim 1.50-1.55$. The anisotropic properties are related to the nematic configuration in the droplets and can therefore be influenced by external electric or magnetic fields. To focus our attention on the effects of the optical anisotropy we shall limit our treatment to cases where multiple scattering can be neglected. In case of submicron nematic droplets this is not a severe limitation because they have relatively small scattering cross sections.

For our starting point we use the results obtained in RGA approximation for differential and total cross section in our recent paper[11]. In Section II we describe our system of droplets and possible director configurations. In Section III we introduce effective cross sections per droplet and the structure factor for the description of the interdroplet interference. Section IV is devoted to the study of pair correlations and their effect on the structure factor. In Section V we calculate effective scattering cross sections in RGA for different structures. In Section VI we define and calculate the attenuation coefficient. In Section VII theoretical results are compared with experimental data.

II. NEMATIC DISPERSION

These materials are the result of polymerization induced phase separation from initially homogeneous solution of liquid crystals and monomers. The dispersions can have relatively uniform droplet sizes,[15,17] with a mean size ranging from 0.1 to 10μm, depending on the concentration of the liquid crystal and polymerization rate.[17] A typical example of an electron microscope picture of a cut-through is shown in Fig. 1.

The equilibrium director configuration of a nematic liquid crystal in a spherical droplet is well known only in large droplets where it can be studied with an optical microscope.[18,19] For submicron droplets there are only theoretical predictions based on the strong anchoring conditions.[20-22] In this paper we will deal with director configurations calculated in the approximation of a single elastic constant $K_1 = K_2 = K_3 = K$ and strong surface anchoring which can be either parallel or orthogonal to the polymer-liquid crystal interface. Further, we neglect a possible spatial dependence of the nematic order parameter. The minimization of the free energy (elastic and external field contributions) results in a nonlinear partial differential equation which is solved using the nonlinear over-relaxation method.[23]

3

The degree of the field induced director alignment in the droplet depends on the strength of the external field. The correlation length[24] $\xi = (k/\Delta\varepsilon\varepsilon_o)^{\frac{1}{2}}/E$ is usually used as a measure of the range of the surface induced ordering in the presence of the external field E. Here $\Delta\varepsilon$ is the anisotropy of the dielectric constant. The solution for parallel anchoring has two point defects in the bipolar structure (see schematic representation in Fig. 2). We introduce the term droplet director N for the direction of the axis of the cylindrical symmetry. In the case of normal surface alignment the solution is a star structure for low fields and configurations with an equatorial disclination[11] line for strong fields.

III. STRUCTURE FACTOR

Neglecting multiple scattering we can write the total scattered electric field at an arbitrary observation point r, where the far field approximation is valid, as a simple sum:

$$E_s(r) = \sum_j E_{sj}(r) e^{i(k-k')\cdot r_j}. \tag{1}$$

Here E_{sj} is the contribution of the jth droplet located at r_j (see Fig. 3). We are assuming that the coherence length of the incident light is very large in comparison to the inter droplet distances. To get a measure of the scattering power we introduce the effective differential cross section per droplet as

$$\frac{d\sigma}{d\Omega} = \frac{r^2}{N} \left| \frac{E_s(r)}{E_o} \right|^2 \tag{2}$$

4

where E_o is the amplitude of the incoming planar wave and N the number of droplets. Substituting Eq. (1) into definition (2) one finds:

$$\frac{d\sigma}{d\Omega} = \frac{r^2}{N} \left[\sum_i \left| \frac{\mathbf{E}_{si}(\mathbf{r})}{E_o} \right|^2 + \sum_{i \neq j} \frac{\mathbf{E}_{si}(\mathbf{r}) \cdot \mathbf{E}_{sj}^*(\mathbf{r})}{E_o^2} e^{i(\mathbf{k} - \mathbf{k}') \cdot (\mathbf{r}_i - \mathbf{r}_j)} \right]. \tag{3}$$

Further, we substitute the summation over different droplets by averaging over possible orientations of anisotropic droplets and as well over different droplet sizes:

$$\frac{1}{N} \sum_j \rightarrow \langle \ \rangle,$$

and get

$$\frac{d\sigma}{d\Omega} = \langle \frac{d\sigma_j}{d\Omega} \rangle + \frac{d\sigma_{()}}{d\Omega} \frac{1}{N} \sum_{i \neq j} e^{i\mathbf{k}_s \cdot (\mathbf{r}_i - \mathbf{r}_j)}. \tag{4}$$

where $d\sigma_{()}/d\Omega$ stands for the cross section corresponding to the average scattered field $<\mathbf{E}_{sj}>$ and $d\sigma_j/d\Omega$ for the differential cross section of jth droplet. We use $\mathbf{k}_s$ for $\mathbf{k}-\mathbf{k}'$. We have taken into account that there is no correlation between droplet position, orientation, and size. Introducing positional pair correlation function[25] $g(\mathbf{r})$ we can write for the case of $N >> 1$:

$$\frac{1}{N} \sum_{i \neq j} e^{i\mathbf{k}_s \cdot (\mathbf{r}_i - \mathbf{r}_j)} = \frac{N}{V} \int g(\mathbf{r}') e^{i\mathbf{k}_s \cdot \mathbf{r}'} dV', \tag{5}$$

where N/V is the number of droplets per unit volume. The Fourier transform of $g(r)$ given by Eq. (5) has a strong forward ($k_s = 0$) part, which in fact does not contribute to the scattering and is usually subtracted.[26] Therefore, we can rewrite Eq. (4) as:

$$\frac{d\sigma}{d\Omega} = \langle\frac{d\sigma_i}{d\Omega}\rangle + \frac{d\sigma_{()}}{d\Omega} G_s(k_s),$$ (6)

where

$$G_s(k_s) = \frac{N}{V} \int g(r') e^{ik_s \cdot r'} dV'.$$ (7)

It is convenient to introduce the structure factor[26,27]

$$F(k_s) = 1 + G_s(k_s) \frac{d\sigma_{()}}{d\Omega} / \langle\frac{d\sigma_i}{d\Omega}\rangle$$ (8)

so that effective differential cross section is given by:

$$\frac{d\sigma}{d\Omega} = \langle\frac{d\sigma_i}{d\Omega}\rangle F(k_s).$$ (9)

In a simple case where all droplets are eigenvalent $F(k_s)$ reduces to

$$F(k_s) = 1 + G_s(k_s).$$ (10)

In the following we are going to discuss possible simple forms of the pair correlation function, which will enable us to get $F(k_s)$.

6

IV. PAIR CORRELATIONS

In principle the pair correlation function could be obtained by electron microscopy, when the spatial position of the droplets are resolved. Usually only a 2D study is performed by observing a reflection on a planar cut through the sample (see Fig. 1). In such a case the apparent pair correlation function $\breve{g}(\rho)$ is related to the $g(r)$ in the following way

$$\breve{g}(\rho) = \frac{1}{4R^2} \int_{-R}^{R} \int_{-R}^{R} g\left(\sqrt{\rho^2 + (z-z')^2}\right) dz\, dz' , \tag{11}$$

where ρ is the interdroplet distance in the plane of cutting. There is no general way of solving this kind of integral equation.[28]

Let us try to illustrate our discussion on a simple example when $g(r)$ is of a square well type (good approximation for diluted dispersions of hard spheres of the same size):

$$g_o(r) = \begin{Bmatrix} 0 & r < b \\ 1 & r \geq b \end{Bmatrix} , \tag{12a}$$

then $b = 2R$ (see Fig. 4a). Inserting Eq. (12a) into (11) one finds

$$\widetilde{g}_o(\rho) = \begin{Bmatrix} (1 - (1 - (\rho/2R)^2)^{\frac{1}{2}})^2 & \rho < b \\ 1 & \rho \geq b \end{Bmatrix} , \tag{12b}$$

where the apparent pair correlation function $\breve{g}_o(\rho)$ differs from g_o for small distances (see Fig. 4b). These kind of differences between $g(r)$ and $\breve{g}(\rho)$ are expected also in more realistic cases.

7

The real $g(r)$ for a nematic droplet dispersion is affected by a size distribution $P(R)$. To see what kind of changes one can expect, we can study the limit of low concentrations where we find:

$$g(r) = \int P(R) g_o(r) \, dR = \int_o^{r/2} P(R) \, dR .$$ (13)

To show the effect of $P(R)$ we choose a simple gamma distribution

$$P(R) = a^\beta \Gamma(\beta)^{-1} R^{\beta-1} e^{-aR}$$ (14)

usually used for the description of the colloid dispersion.[29] It can qualitatively describe some nematic dispersions as well.[17] Here $\Gamma(\beta)$ is a complete gamma function. Parameters a and β are simply related to $\langle R \rangle$ and $\sigma_R = (\langle R^2 \rangle - \langle R \rangle^2)^{\frac{1}{2}}$ by relations

$$\langle R \rangle = \beta/a$$ (15a)

and

$$\sigma_R = \frac{\sqrt{\beta}}{a} .$$ (15b)

In Fig. 5 it is shown how the distribution changes with σ_R for a chosen $\langle R \rangle$.

Introducing distribution (14) into Eq. (13) one finds

$$g(r) = \gamma\left(\beta, \frac{ar}{2} \right) / \Gamma(\beta)$$ (16)

8

when $\gamma(\beta, ar/2)$ is the incomplete gamma function. The resulting low concentration pair correlation function is shown in Fig. 4(c) for $\sigma_R = <R>/2$.

The pair correlation functions $g(r)$ given by Eq. (12) or Eq. (16) are not suitable for the description of higher concentrations. One must use experimental data or simulate $g(r)$ on a computer or use a Percus-Yevick type approach developed for hard spheres. The last approach was explained in detail by Vrij.[24,30]

Let us calculate the structure factor for our simple case given by Eq. (12). Introducing

$$u(x) = \frac{3}{x^3}\left(sinx - x\,cosx\right) \tag{17}$$

one can write

$$G_s = -8\,C_D\,u(2k_sR). \tag{18}$$

Where C_D is the volume fraction occupied by droplets. If all droplets are equally oriented follows

$$F(k_s) = 1 - 8\,C_D\,u(2k_sR). \tag{19}$$

One can see that only low C_D ($< 1/8$) gives physically reasonable results. In Fig. 6 $F(k_s)$ is illustrated for several C_D. The forward scattering is reduced due to the complete randomness of the droplet positions. The low concentration reduction where Eq. (19) can be used is proportional to C_D. After our treatment of single droplet scattering we shall be able to see how $F(k)$ is influenced by the distribution of sizes.

V. LIGHT SCATTERING IN RGA

We are going to use the results of Ref. 11 where in RGA differential and total cross sections have been evaluated.

Using the scattering matrix representation (1) we can write (see Ref. 11) the scattered electric field as:

$$
\begin{bmatrix} (E_s)_{\shortparallel} \\ (E_s)_{\perp} \end{bmatrix} = \sum_j \begin{bmatrix} S_{\shortparallel\shortparallel j} & S_{\shortparallel\perp j} \\ S_{\perp\shortparallel j} & S_{\perp\perp j} \end{bmatrix} \begin{bmatrix} e \cdot i_{\shortparallel} \\ e \cdot i_{\perp} \end{bmatrix} E_o \, e^{i(\mathbf{k}-\mathbf{k'})\cdot \mathbf{r}_j} \frac{e^{ikr}}{kr} , \qquad (20)
$$

where r is the distance to the observer, e is the polarization unit vector, $i_{\shortparallel}$ and $i_{\perp}$ are unit vectors perpendicular to k, $\shortparallel$ stands for parallel to the scattering plane, and $\perp$ stands for the direction orthogonal to it (see Fig. 3). The scattering matrix is:

$$
\underline{\underline{S}}_j = \frac{(kR)^2}{3} \begin{bmatrix} i'_{\shortparallel} \cdot (D_j i_{\shortparallel}) & i'_{\shortparallel} \cdot (D_j i_{\perp}) \\ i_{\perp} \cdot (D_j i_{\shortparallel}) & i_{\perp} \cdot (D_j i_{\perp}) \end{bmatrix} \qquad (21)
$$

When $i_{\shortparallel}'$ is the unit vector parallel to the scattering plane and orthogonal to k' and D_j is the 3D Fourier transform of the $\varepsilon_m^{-1}\underline{\varepsilon}$-1. Here ε_m is the dielectric constant of the isotropic polymeric matrix and $\underline{\varepsilon}$ is the dielectric constant of the nematic phase oriented with the main principal axis parallel to the local director n. The corresponding principal values are $\varepsilon_{\shortparallel}$ and $\varepsilon_{\perp}$. Here we are going to neglect possible spatial variation of the nematic order parameter in the droplet. Limiting our treatment to spherical droplets we can, according to I, express D as:

$$
\underline{D}(kR) = 1\zeta u(k_s R) + \eta \sum_{j=0,\pm 1,\pm 2} \beta_j \upsilon_j (Rk_{s\rho},\phi_s,Rk_{sz}) , \qquad (22)
$$

where

$$\zeta = Tr(\underline{\varepsilon})/3\varepsilon_m - 1 \tag{23a}$$

$$\eta = \frac{\varepsilon_\parallel - \varepsilon_\perp}{3\varepsilon_m}, \tag{23b}$$

$$\underline{\beta}_o = \begin{pmatrix} 1 & 0 & 0 \\ 0 & 1 & 0 \\ 0 & 0 & 2 \end{pmatrix}, \quad \underline{\beta}_{+1} = \begin{pmatrix} 0 & 0 & 1 \\ 0 & 0 & 0 \\ 1 & 0 & 0 \end{pmatrix}, \quad \underline{\beta}_{-1} = -\begin{pmatrix} 0 & 0 & 0 \\ 0 & 0 & 1 \\ 0 & 1 & 0 \end{pmatrix},$$

$$\underline{\beta}_{+2} = \begin{pmatrix} 1 & 0 & 0 \\ 0 & 1 & 0 \\ 0 & 0 & 0 \end{pmatrix}, \quad \underline{\beta}_{-2} = -\begin{pmatrix} 0 & 1 & 0 \\ 1 & 0 & 0 \\ 0 & 0 & 0 \end{pmatrix}, \tag{24}$$

$$\upsilon_o(Rk_{s\rho}, Rk_{sz}) = \frac{4\pi}{V} \int_o^R \int_o^{\rho(z)} (1 - \frac{3}{2}\sin^2\theta_n) J_o(k_{s\rho}\rho_n)\cos(k_{sz}z_n)\rho_n d\rho_n dz_n, \tag{25a}$$

$$\upsilon_{\pm 1}(Rk_{s\rho}, \phi_s, Rk_{sz}) = \frac{4\pi}{V} \begin{Bmatrix} \cos\phi_s \\ \sin\phi_s \end{Bmatrix} \int_o^R \int_o^{\rho(z)} \sin2\theta_n J_1(k_{s\rho}\rho_n)\sin(k_{sz}z_n)\rho_n d\rho_n dz_n \tag{25b}$$

$$\upsilon_{\pm 2}(Rk_{s\rho}, \phi_s, Rk_{sz}) = \frac{4\pi}{V} \begin{Bmatrix} \cos2\phi_s \\ \sin2\phi_s \end{Bmatrix} \int_o^R \int_o^{\rho(z)} \sin^2\theta_n J_2(k_{s\rho}\rho_n)\cos(k_{sz}z_n)\rho_n d\rho_n dz_n. \tag{25c}$$

Here J_0, J_1, and J_2 are Bessel functions. The components of the wave vector $\mathbf{k}_s$ written in terms of angles θ, δ, and γ (see Fig. 7) are

$$k_{s\rho} = k\left\{(1-\cos\delta)\left[\cos^2\theta\,(1-\cos\delta) + 2(1-\sin\delta\cos\theta\cos\gamma) + (1+\cos\delta)\sin^2\theta\cos^2\gamma\right]\right\}^{\frac{1}{2}}, \tag{26a}$$

11

$$k_{sz} = k \left[cos\theta(1 - cos\delta) - sin\delta sin\theta cos\gamma \right],$$

$$(26b)$$

$$\phi_s = arctan \frac{-sin\delta sin\gamma}{sin\delta cos\theta cos\gamma + sin\theta(1 - cos\delta)},$$

$$(26c)$$

and its absolute value is given by

$$k_s = 2k \, sin \frac{\delta}{2}.$$

$$(27)$$

The differential cross section of the jth droplet can be written as

$$\left. \begin{array}{c} \frac{d\sigma}{d\Omega}\Big|_{\parallel} \\ \frac{d\sigma}{d\Omega}\Big|_{\perp} \end{array} \right\} = \frac{k^4 R_j^6}{9} \left\{ \begin{array}{c} |\mathbf{i'}_{\parallel} \cdot (\underline{\mathbf{D}}_j \mathbf{e})|^2 \\ |\mathbf{i}_{\perp} \cdot (\underline{\mathbf{D}}_j \mathbf{e})|^2 \end{array} \right.$$

$$(28)$$

To get the effective cross section we must calculate

$$\langle \frac{d\sigma_j}{d\Omega} \rangle = \frac{k^4}{9} \langle R_j^6 \left[\left| \mathbf{i'}_{\parallel} \cdot \left(\underline{\mathbf{D}}_j \mathbf{e} \right) \right|^2 + \left| \mathbf{i}_{\perp} \cdot \left(\underline{\mathbf{D}}_j \mathbf{e} \right) \right|^2 \right] \rangle$$

$$(29)$$

and

$$\frac{d\sigma_{\langle\rangle}}{d\Omega} = \frac{k^4}{9} \left[\left| \langle R_j^3 \, \mathbf{i'}_{\parallel} \cdot \left(\underline{\mathbf{D}}_j \mathbf{e} \right) \rangle \right|^2 + \left| \langle R_j^3 \, \mathbf{i}_{\perp} \cdot \left(\underline{\mathbf{D}}_j \mathbf{e} \right) \rangle \right|^2 \right].$$

$$(30)$$

The average $< >$ includes averages over size and over the possible orientation of droplet directors. In general $\underline{\mathbf{D}}$, which is related to the director configuration, depends on the droplet radius, so that all these averaging must be performed numerically. If the spread in droplet size is small, $\sigma_R \leq <R>$, we can take into account the fact that in Eq. (29) the dependence of $\underline{\mathbf{D}}$ on radius is much weaker than

12

the dependence of the factor R^6. Limiting to such cases, we can separate the averaging over size $< >_R$ from the averaging over droplet director orientation $< >_\Omega$ and get:

$$\langle \frac{d\sigma_j}{d\Omega} \rangle = \frac{k^4}{9} \langle R^6 \rangle \left[\langle \left| \mathbf{i'_\parallel} \cdot \left[\underline{\mathbf{D}}_j\big(\langle R \rangle \mathbf{k}_s\big) \mathbf{e} \right] \right|^2 \rangle_\Omega + \right.$$

$$\left. + \langle \left| \mathbf{i'_\perp} \left[\underline{\mathbf{D}}_j\big(\langle R \rangle \mathbf{k}_s\big) \mathbf{e} \right] \right|^2 \rangle_\Omega \right], \tag{31}$$

and

$$\frac{d\sigma_{\langle\rangle}}{d\Omega} = \frac{k^4}{9} \langle R^3 \rangle^2 \left[\left| \mathbf{i'_\parallel} \cdot \langle \underline{\mathbf{D}}_j\big(\langle R \rangle \mathbf{k}_s\big) \mathbf{e} \rangle_\Omega \right|^2 + \left| \mathbf{i_\perp} \cdot \langle \underline{\mathbf{D}}_j\big(\langle R \rangle \mathbf{k}_s\big) \mathbf{e} \rangle_\Omega \right|^2 \right]. \tag{32}$$

In order to be able to calculate the attenuation constant we must first calculate the total cross section:

$$\sigma = \int \langle \frac{d\sigma_j}{d\Omega} \rangle \langle F(k_s) \rangle_R \, d\cos\delta \, d\alpha , \tag{33}$$

where $<F>_R$ stands for the structure factor with the pair correlations averaged over droplet sizes. In the following we are going to treat some special cases.

i) <u>Droplets With Radial Director Configuration</u>. Using results from I and Eq. (19) one finds:

$$\sigma = \frac{\pi}{9} k^4 <R^6> \int \left\{ (1 - \cos^2\delta) \zeta^2 u^2\big(k_s\langle R \rangle\big) - 2\Big(1 + \frac{3}{2}\cos\delta - \frac{1}{2}\cos^2\delta\Big) \zeta\eta \, u\big(k_s\langle R \rangle\big) v_o\big(k_s\langle R \rangle\big) \right.$$

13

$$+ \eta^2 v_o^2 \Big(k_s (R) \Big) \Big[1 + \frac{1}{4} (3 + \cos\delta)^2 \Big] \Big\} \; F(\mathbf{k}_s) \; d(\cos\delta). \qquad (34a)$$

when

$$F(\mathbf{k}_s) = \Big[1 + G_s(\mathbf{k}_s) {<}R^3{>}^2 / {<}R^6{>} \Big], \qquad (34b)$$

where in this case v_o given by Eq. (25a) reduces to

$$v_o(x) = \frac{3}{x^3} \Big\{ 4 \sin x - x \cos x - 3 Si x \Big\}. \qquad (35)$$

Let us first consider the case where all droplets have the same size $({<}R^6{>} = {<}R^3{>}^2 = R_o^6)$ and G_s is given by Eq. (18). Figure 8a shows the effect of the volume fraction occupied by droplets on the differential cross section given by the function under the integral Eq. (34). By increasing C_D backward scattering is increasing and forward scattering is decreasing. It reflects the constructive interference of light scattering by the closest droplets. The effect of C_D on the effective total cross section is shown on Fig. 9a. It should be stressed that here we used low concentration approximation for $g(r)$. In case of droplet size distribution the interdroplet interference is strongly reduced. For the case $\sigma_R = R/2$ presented in Fig. 5 we have ${<}R^3{>}^2/{<}R^6{>} = 5/21$ that reduces the interference term in Eq. (34) for a factor ≈ 4. In this consideration we neglect changes in $G_s(k_s)$ which are less drastic.

ii) <u>Droplets Oriented in a Strong Field</u>. Here we are going to illustrate the case of k‖N (also ‖ external field) where expressions become particularly simple. One finds

14

$$\sigma = \frac{\pi}{9} k^4 \langle R \rangle^6 (\zeta - \eta)^2 \int (1 + \cos^2\delta) \, u^2\left(k_s \langle R \rangle\right) F(k_s) \, d\cos\delta \,. \qquad (36)$$

The behavior of $d\sigma/d\Omega$ for systems with uniform size droplets where $F(k_s)$ is given by Eq. (34b) is shown on Fig. 8b and is similar to the behavior of the radial case. The same is true for the total cross section (see Fig. 9b).

iii) <u>Randomly Distributed Droplet Directors</u>. Here we assume that there is no external field and that droplet structures are bipolar. Unfortunately $<d\sigma/d\Omega>$ given by Eq. (31) cannot be simplified. The whole averaging process must be performed numerically. On the other hand, the evaluation of $d\sigma_{()}/d\Omega$ reduces to the evaluation of $<\underline{D}_j(<R>k_s)>$ and further to

$$\langle \varepsilon/\varepsilon_m - 1 \rangle = 1 \, (2\varepsilon_\perp + \varepsilon_\parallel)/\varepsilon_m - 1 \,, \qquad (37)$$

when the complete randomness of the distribution has been taken into account. The resulting

$$\langle D \rangle = 1 \zeta \, u\left(\langle R \rangle k_s \right) \qquad (38)$$

corresponds to the isotropic droplet with average ε, so that we can write

$$\frac{d\delta_{()}}{d\Omega} = \frac{k^4}{9} \langle R^3 \rangle^2 \zeta^2 \left(\cos^2\delta\cos^2 a + \sin^2 a \right) u^2\left(\langle R \rangle k_s \right). \qquad (39)$$

The behavior of the resulting effective differential cross section is shown in Fig. 8c.

VI. ATTENTUATION OF THE LIGHT

The decrease in the intensity of the light beam j after passing the distance dz in our media is given by:

$$dj = -j\sigma \frac{N}{V} dz.$$ (40)

Introducing the average volume of a droplet $3\pi <R^3>/4$ we get:

$$j = j_o e^{-\mu z}.$$ (41)

where the attenuation coefficient is given by

$$\mu = C_D \frac{3\sigma}{4\pi \langle R^3 \rangle}.$$ (42)

The validity of Eq. (41) is limited to the situation where the contribution of the single or multiple scattered light registered by the detector is small compared to the contribution of the attenuated direct beam. For small droplets, $kR \lesssim 1$ where the scattering is not predominantly forward, we estimate the limitation on j/j_o in the following way:

$$\frac{j}{j_o} >> \frac{\Delta\Omega}{4\pi}$$ (43)

where $\Delta\Omega$ is the solid angle of the detector. Here we assume that the scattered light is coming uniformly from all directions but only $\Delta\Omega/4\pi$ of it is registered by the

16

detector. In case of large droplets, $kR > 1$, the scattering is predominantly forward so that limitations are more severe

$$\frac{j}{j_o} >> \frac{\Delta\Omega_s}{\Delta\Omega_o} , \qquad (44)$$

where $\Delta\Omega s$ is the solid angle into which the dominant part of the light is scattered.[31]

VII. EXPERIMENTAL RESULTS

To experimentally examine the theoretical results, samples were made using the liquid crystal E7 (BDH Chemicals, England) and the epoxy resin Bostik (Bostik Sp.A., Italy). The preparation involves phase separation of a liquid crystal rich phase from our initially homogeneous mixture, as described elsewhere.[32] Samples were prepared sandwiching the uncured material between two conducting (In/Sn oxide coated) glasses and allowing the phase separation to occur at a definite temperature. The spacing between the glasses was controlled using Alufrit spacers (Atomergic Chemicals, NY) and chosen to be ~60 μm, unless otherwise specified. The N-I transition temperature of the liquid crystal rich phase increases for about 2 weeks after the sample preparation, to reach a constant value ~2°C lower than the transition temperature in the pure E7. Light transmission measurements were then taken only after the cure of the materials was completed.

Since for our light attenuation experiments, materials with small droplets were needed, samples were chosen with an average ratio of $<R> \simeq 0.1 \pm 0.05$ μm, and $<R> = 0.13 \pm 0.1$ μm. These sizes were measured on the samples used for the experiments by scanning electron microscopy (see Fig. 1). The relatively large error on the detection of the droplets dimensions is a consequence of their small size which is at the limit of detection for the SEM technique on these materials. While for the

17

samples in the larger size droplets, SEM allowed an estimate of the droplets volume fraction, $C_D \simeq 0.1$. In the samples with small droplets only a rough size determination was possible, but not enough details were accessible for an evaluation of C_D. Although characterization of samples with larger droplets would have been easier, their use would have led us out of the approximation range we deal with in this paper.

Figure 10 shows the dependence of transmitted light on the thickness of the nematic embedding polymeric material when no electric field is applied. The light source used was an He-Ne laser (Spectra-Physics). The transmitted intensity shows an exponential dependence on the thickness, as described by Eq. (41), in this case where droplets are small ($<R> \sim 0.1\,\mu m$).

In Fig. 11 the dependence of the measured attenuation coefficient on the reciprocal wavelength is shown. As expected for our approximation, $<R> \leq 1$, the fourth power dependence of the attenuation coefficient on k ($\mu\alpha\sigma$) is followed rather well. Theroretical curves are derived using the expressions valid for a random distribution of droplets (section V-III) The indices of refraction used in these expressions for E7 were the ones measured at room temperature: $n_o = 1.522$ and $n_e = 1.746$. For the index of refraction of the polymeric medium we could not use the value measured in the pure epoxy material because we know that a certain amount of liquid crystal is retained in the polymer matrix as a consequence of the preparation technique, having as an effect an overall increase in the refraction index. Since we estimate for our samples that about 10% of the total weight has to be accounted for by liquid crystal solution "dissolved" in the polymer medium, the index of refraction used for the embedding matrix was taken to be $n_m = 1.561$ which is the value measured at room temperature for a sample cured from an E7/Bostik 1:9 mixture.

Figure 12 shows the dependence of the transmitted intensity through the material as a function of an external electric field. Again the light source is an He-Ne laser. Theoretical calculations of the field dependence of light transmission would require a much more detailed analysis, which is beyond the aim of this work and in addition, to be compared with experiments, would require much better sample characterization (droplet size and shape). Theoretical results can easily be obtained only in both limiting cases of no applied field and very high field. The calculated values $\mu(E=0)=0.019$ μm^{-1} and $\mu(strong\ E)=0.0017$ μm^{-1}, are in good agreement with experimental measurements (see Fig. 12).

VII. CONCLUSIONS

We have shown how the attenuation of the light beam in the polymeric dispersion of submicron nematic droplets can be well explained in terms of the Rayleigh-Gans approximation. The possible effect of the inter droplet interference was theoretically analyzed. It was shown that it has minor effect on total cross section, but is crucial for a study of the distribution of the scattered light. We have calculated the effective cross sections for three simple configurations.

The averaging process was separated into angular and size part, which is allowed for the cases with relatively well defined droplet size. Theoretical results are compared to some experimental data obtained from oriented and random droplets dispersed in thin films.

REFERENCES

1. See, for instance, H.C. van de Hulst, *Light Scattering by Small Particles* (Wiley, New York, 1957).

2. M. Kerker, *The Scattering of Light and Other Electromagnetic Radiation* (Academic Press, New York, 1969).

3. C.F. Bohren and D.R. Hoffman, *Absorption and Scattering of Light by Small Particles* (Wiley, New York, 1983).

4. G. Mie, "Beiträge zur Optik Truben Medien, Speciell Kolloidaler Metal-lösungen," Ann. Phys. **25**, 377-445 (1908).

5. S. Asano and G. Yamamoto, "Light Scattering by a Spheroidal Particle," Appl. Opt. **14**, 29-49 (1975).

6. Lord Rayleigh, "On the Diffraction of Light by Spheres of Small Relative Index," Proc. Roy. Soc. **A90**, 219-225 (1914).

7. R. Gans. Ann. Phys. **76**, 29 (1925).

8. M.B. Rhodes and R.S. Stein, "Scattering of Light from Assemblies of Oriented Rods," J. Polym. Sci. A **2**, 1539-1558 (1969).

9. M. Matsuo, K. Kakei, Y. Magaoka, F. Ozaki, M. Murai, and T. Ogita, "A Light Scattering Study of Orientation of Liquid Crystalline Rodlike Textures of Poly(γ-benzyl-L-glutamate) in an Electric Field by Saturation Electric Birefringence Method," J. Chem. Phys. **75**, 5911-5924 (1981).

10. J.V. Champion, A. Killey, and G.H. Meeten, "Small-angle Polarized Light Scattering by Spherulites," J. Polym. Sci., Polym. Phys. Ed. **23**, 1467-1476 (1985).

11. S. Žumer and J.W. Doane, "Light Scattering from a Small Nematic Droplet," Phys. Rev. **34**, 3373-3386 (1986).

12. A. Vrij, J.W. Jansen, J.K.G. Dhont, C. Pathmamanoharan, M.M. Kops-Werkhosen, and H.M. Funant, "Light Scattering of Colloidal Dispersions in Non-

polar Solvents at Finite Concentrations," Faraday Discuss. Chem. Soc. **76**, 19-35 (1983).

13. J.B. Hayten, "Concentrated Colloidal Dispersions Viewed as One-component Macrofluids," Faraday Discuss. Chem. Soc. **76**, 7-17 (1983).

14. H.C. van de Hulst, *Multiple Light Scattering* (Academic Press, NY, 1980).

15. J.W. Doane, N.A. Vaz, B.-G. Wu, and S. Žumer, "Field Controlled Light Scattering from Nematic Microdroplets," Appl. Phys. Lett. **48**, 269-271 (1986).

16. J. Fergason, "Polymer Encapsulated Liquid Crystals for Display and Light Control Applications," SID International Symposium Digest of Technical Papers, **16**, 68-70 (1985).

17. J. West, "Phase Separation of Liquid Crystals in Polymers," Mol. Cryst. Liq. Cryst. (to appear).

18. S. Candau, P. LeRoy, and F. Debeauvais, "Magnetic Field Effects in Nematic and Cholesteric Droplets Suspended in an Isotropic Liquid," Mol. Cryst. Liq. Cryst. **23**, 283-297 (1973).

19. G.E. Volovik and O.D. Lavrentovich, "Topological Dynamics of Defects: Boojums in Nematic Drops," Zh. Eksp. Teor. Fiz. **85**, 1997-2010 (1983); Sov. Phys. JETP **58**, 1159-1166 (1983).

20. P.S. Drzaic, "A New Director Alignment for Droplets of Nematic Liquid Crystals with Low Bend-to-splay Ratio," Mol. Cryst. Liq. Cryst. (to be published).

21. E. Dubois-Violette and O. Parodi, "Emulsions Nematiques. Effects de Champ Magnetiques et Effects Piezoelectriques," J. Phys. C4, 57-64 (1969).

22. R.D. Williams, "Two Transitions in Tangentially Anchored Nematic Droplets," J. Phys. A: Math. Gen. **19**, 3211-3222 (1987).

23. W.F. Ames, *Numerical Methods for Partial Differential Equations* (Academic Press, NY, 1977).

24. P.G. de Gennes, *The Physics of Liquid Crystals* (Clarendon Press, Oxford, 1974).

25. C.A. Croxton, *Introduction to Liquid State Physics* (Wiley, New York, 1975).

26. G. Parod, in *Small Angle X-ray Scattering*, eds. O. Glatter and O. Krotky (Academic Press, New York, 1982), pp. 17-52.

27. P. van Beurten and A. Vrij, "Polydispersity Effects in the Small-angle Scattering of Concentrated Solutions," J. Chem. Phys. **74**, 2744-2748 (1981).

28. F. Smithies, *Integral Equations* (Cambridge University Press, Cambridge, 1958).

29. P. Mittelbach, "Kolloide und Natürliche Makromolecule," Kolloid Z. Z. Polym. **206**, 152-159 (1965).

30. D. Frenkel, R.J. Vos, C.G. de Kruij, and A. Vrij, "Structure Factors of Polydispersed Systems of Hard Spheres: A Comparison of Monte Carlo Simulations and Percus-Yevick Theory," J. Chem. Phys. **84**, 4625 (1986).

31. S. Žumer, "Light Scattering from Nematic Droplets: Anomalous Diffraction Approach," Phys. Rev. A (to appear).

32. B.-G. Wu, J.L. West, and J.W. Doane, "Angular Discrimination of Light Transmission Through Polymer Dispersed Liquid Crystal Films," J. Appl. Phys. **62**, 3925-2931 (1987).

FIGURE CAPTIONS

Fig. 1   Electron scanning microscope picture of the cut-through of a typical sample.

Fig. 2   Schematic presentation of bipolar (a), radial (b), and strongly oriented (c) nematic configuration ($R/\xi \sim 14$).

Fig. 3   Schematic presentation of the scattering on a droplet dispersion.

Fig. 4   Pair correlation function $g(r)$ for diluted dispersion of hard spheres with radia R_o(a), apparent pair correlation function $\bar{g}(\rho)$ given by Eq. (11) (b), and $g(r)$ for distribution given by Eq. (14) with $<R> = R_o$ and $\sigma_R = R_o/2$ (c).

Fig. 5   Droplet size distribution described by Eq. (14) is shown for a chosen $<R>$ and several σ_R (c).

Fig. 6   Structure factor for equal size droplet dispersion as a function of volume fraction (C_D) occupied by droplets.

Fig. 7   Schematic presentation of the scattering geometry for a single droplet with all notation used in the text.

Fig. 8   Effective differential cross section *vs* scattering angle is shown for (a) droplets with radial structure, (b) oriented droplets, and (c) randomly oriented bipolar droplets. The volume fraction occupied by droplets is varied as well. kR is taken to be 1.5.

Fig. 9   Total cross section as a function of kR is shown for (a) droplets with radial structure, (b) oriented droplets, and (c) randomly oriented bipolar droplets.

Fig. 10   The intensity of the light *vs* thickness of the polymeric dispersion film. Results are already corrected for the effect of surface reflections.

Fig. 11   The experimental dependence of the attenuation coefficient on the wavelength of light is shown.
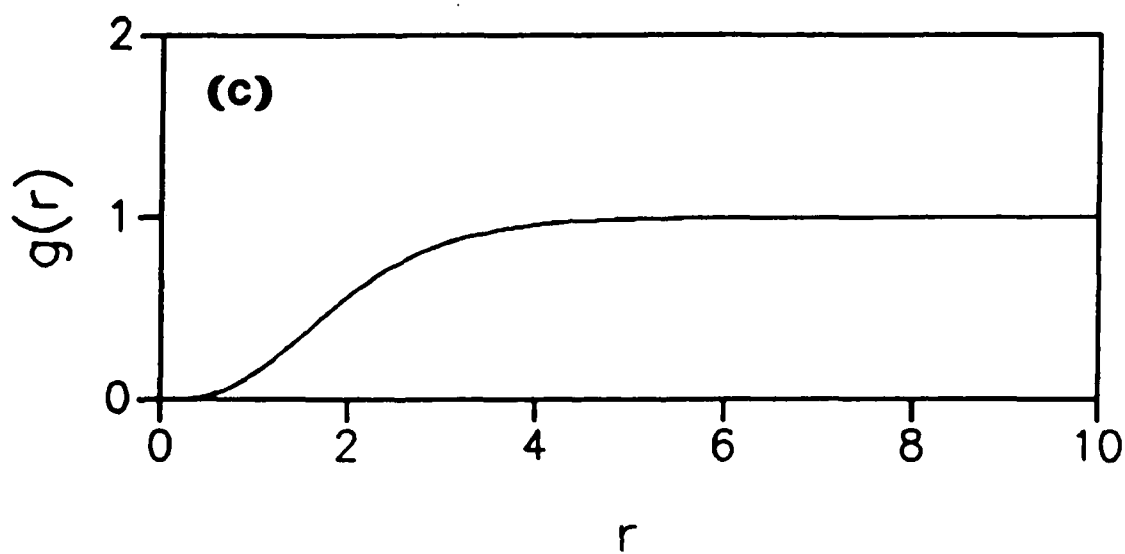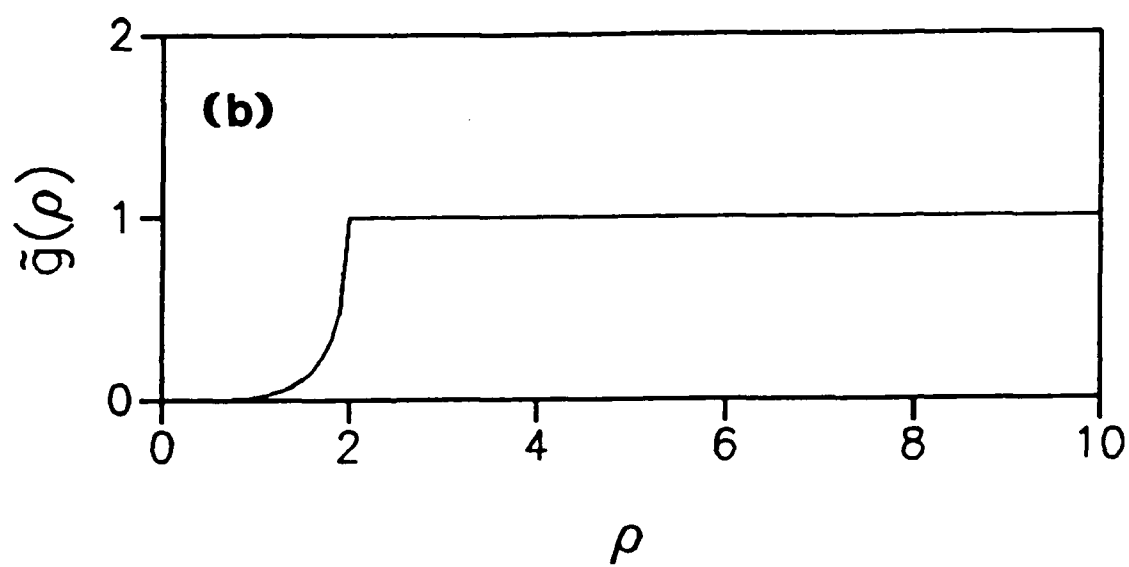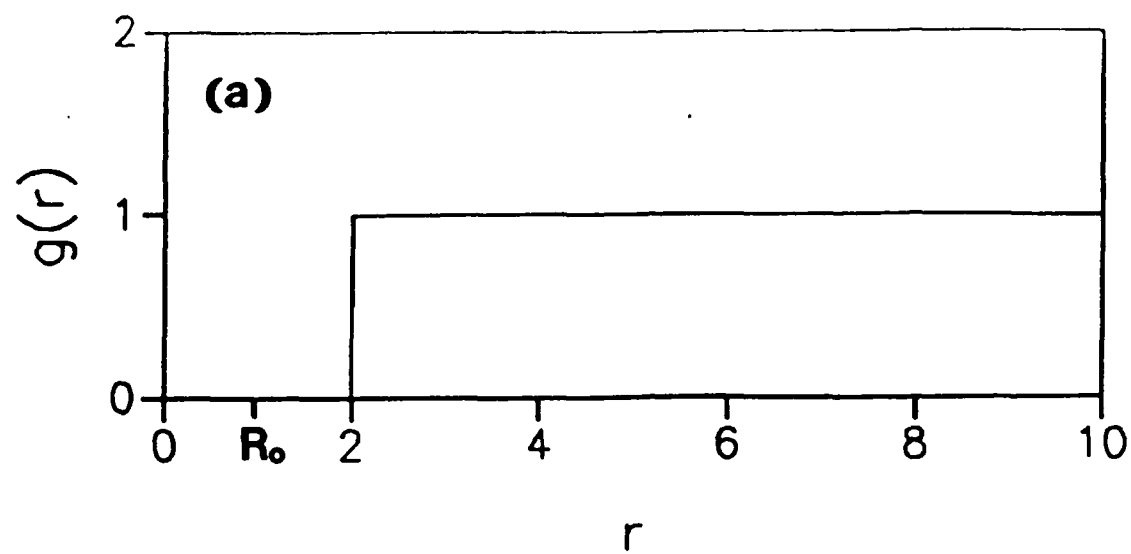
Fig. 12   The experimentally determined attenuation coefficient as a function of the external electric field is shown.
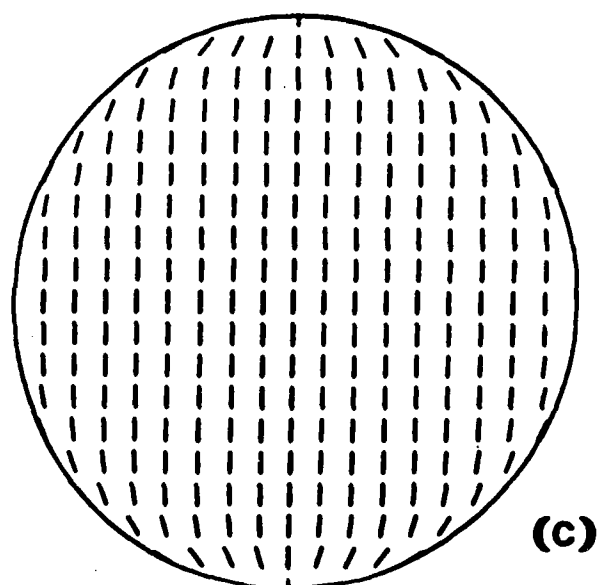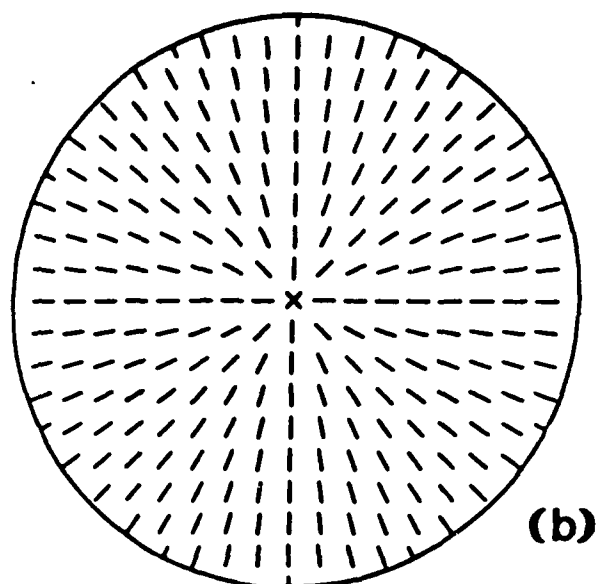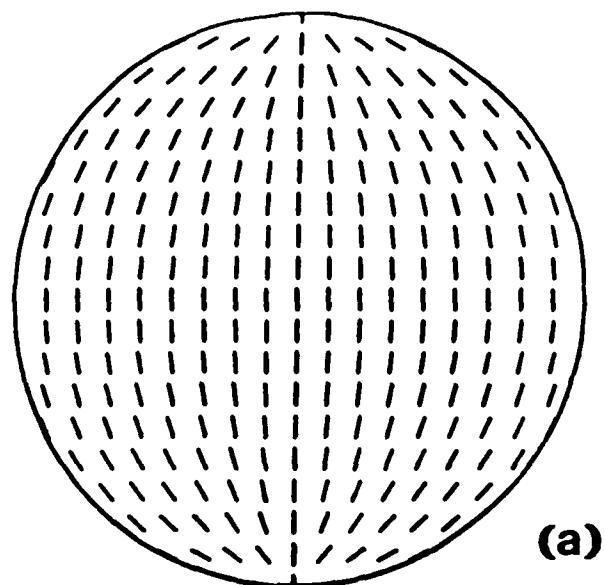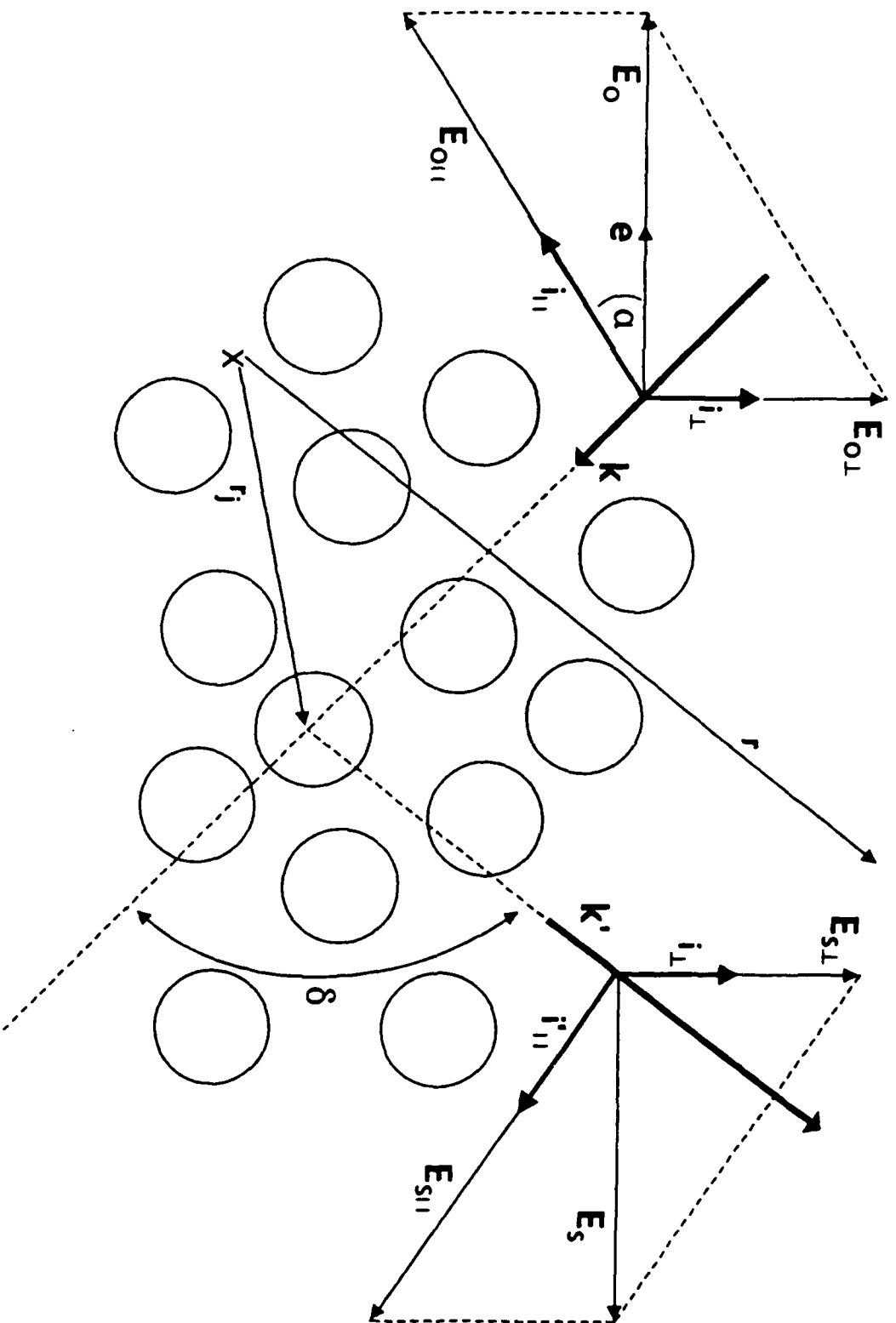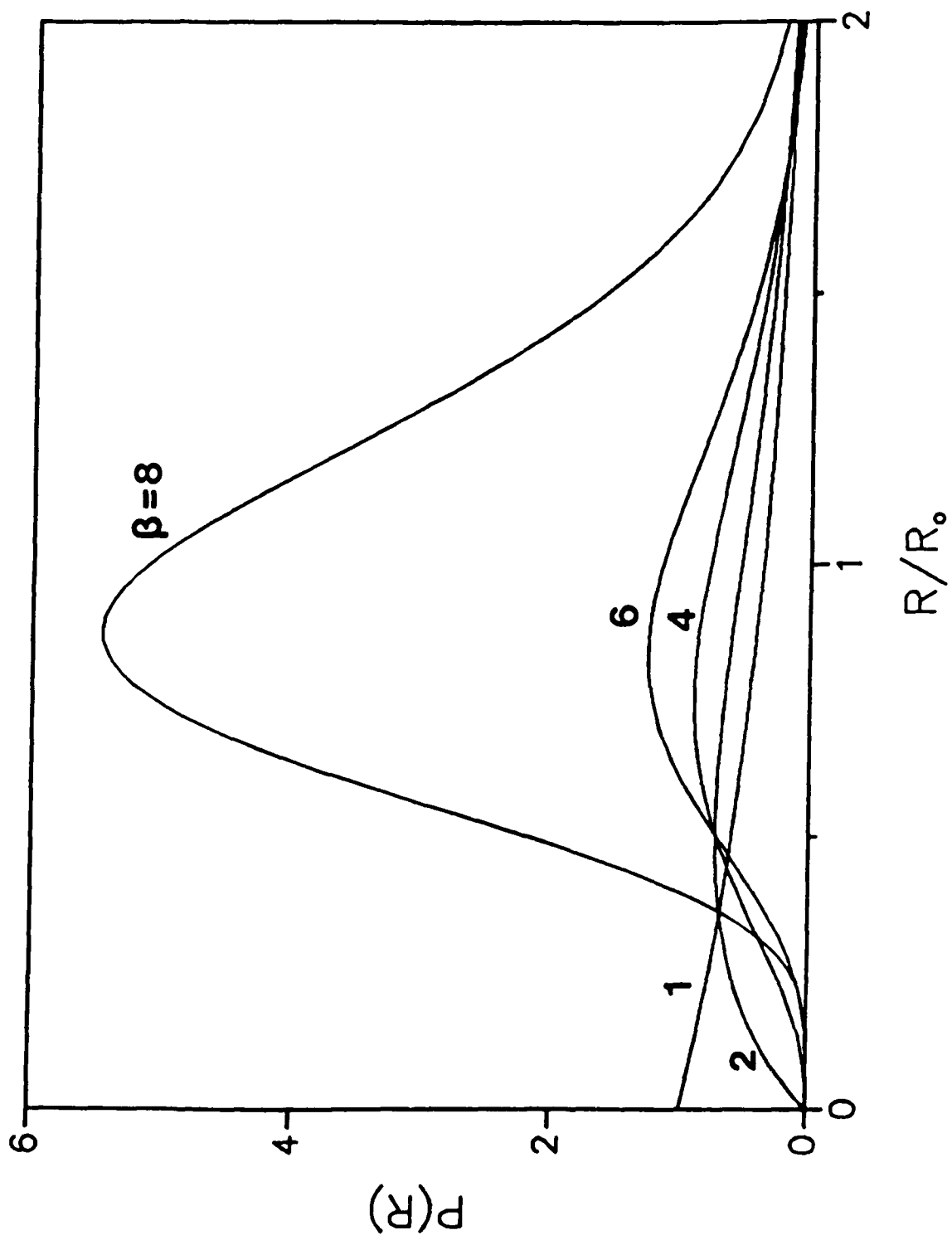
X3600   4001   10.0U

Zumer et al.
- Fig. 1

(a)

(b)

(c)
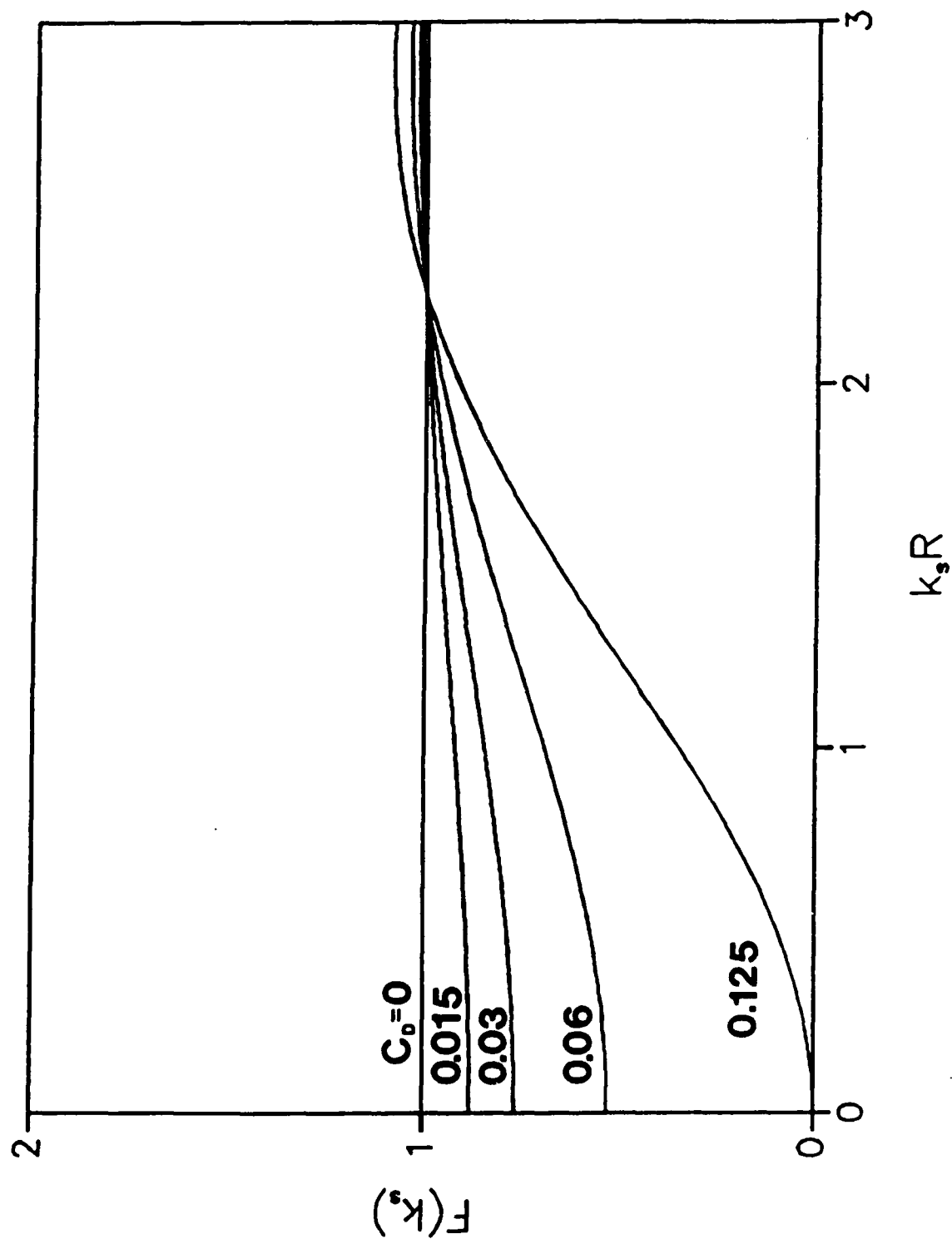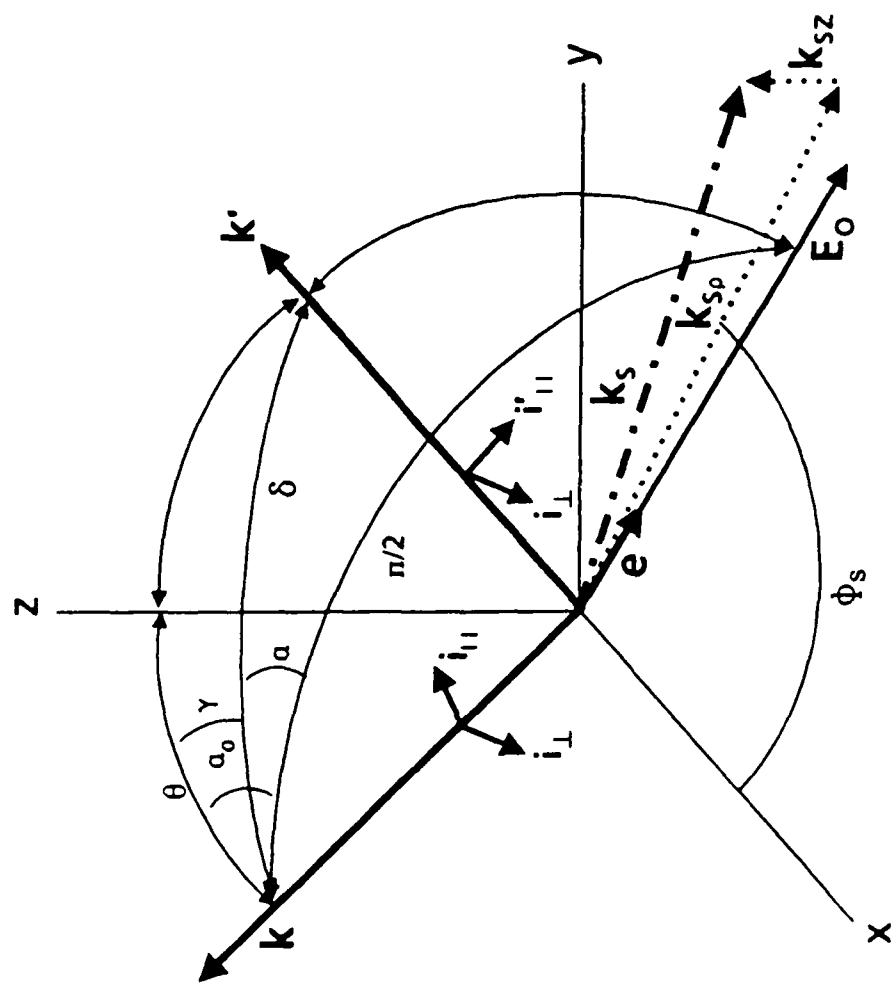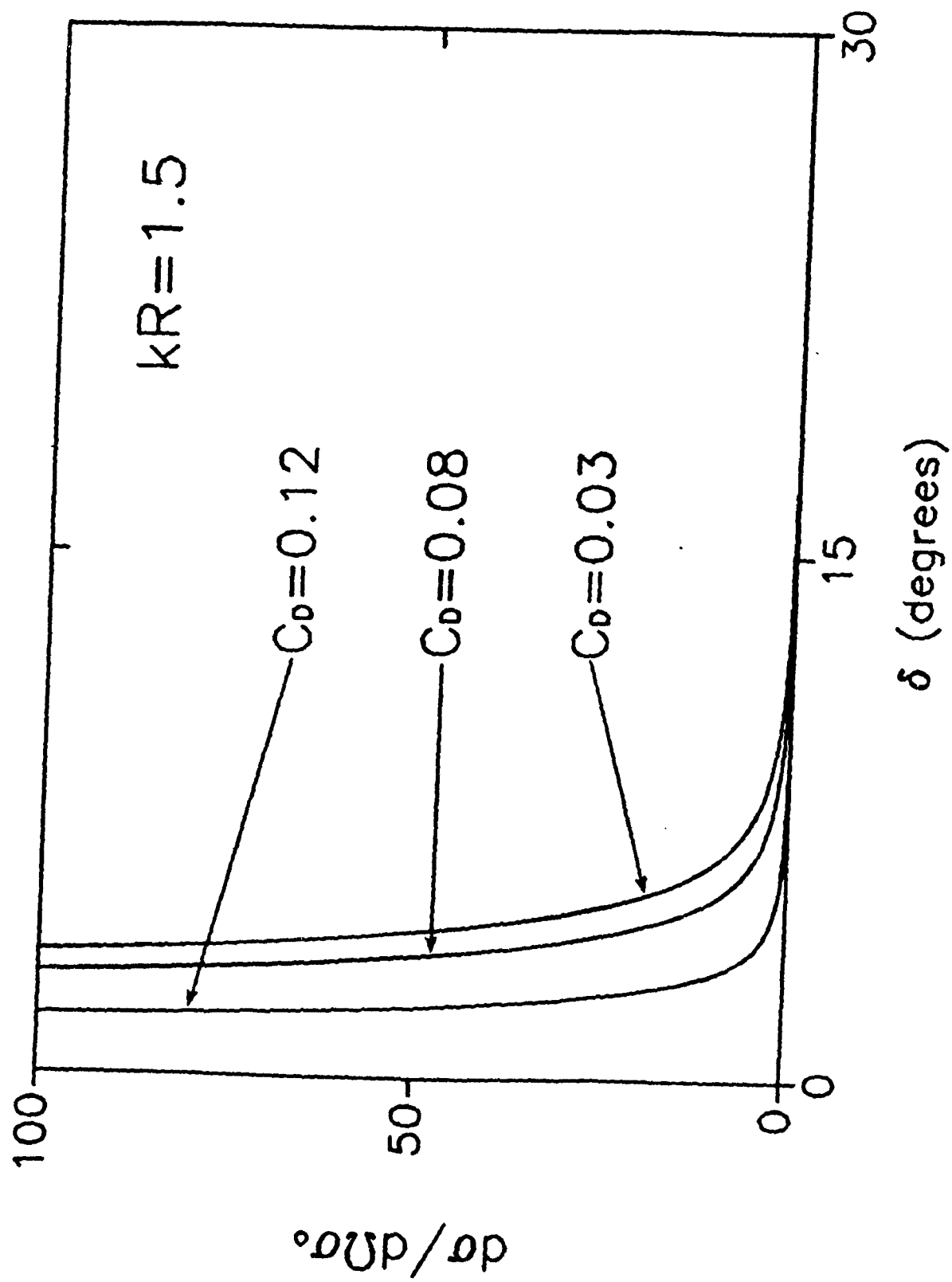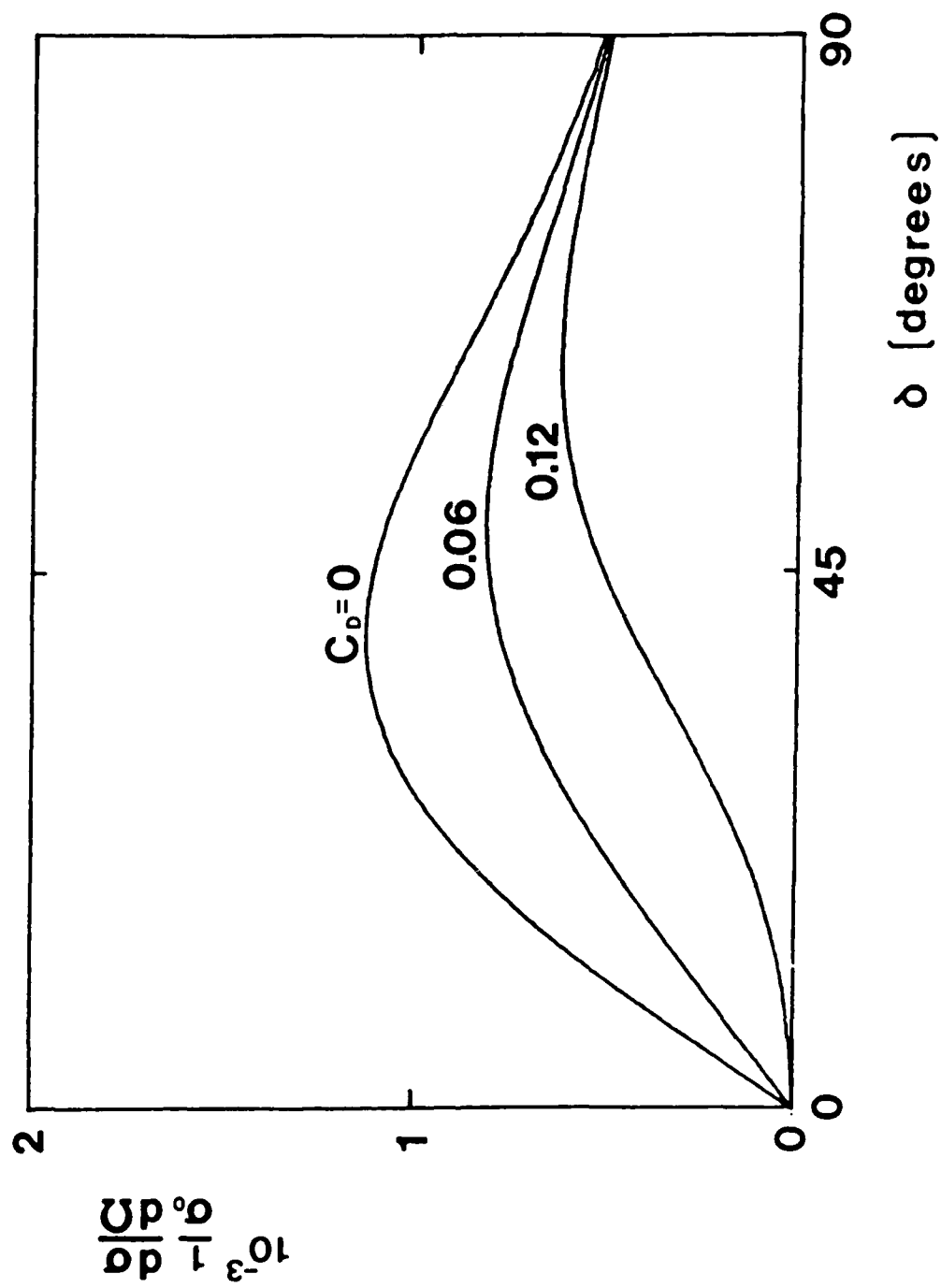
Zumer et al.
Fig. 2

Zumer et al.
Fig. 3

β=8

6

4

1

2

R/R₀

P(R)

Zumer et al.
Fig. 7

kR=1.5

$C_D=0.12$

$C_D=0.08$
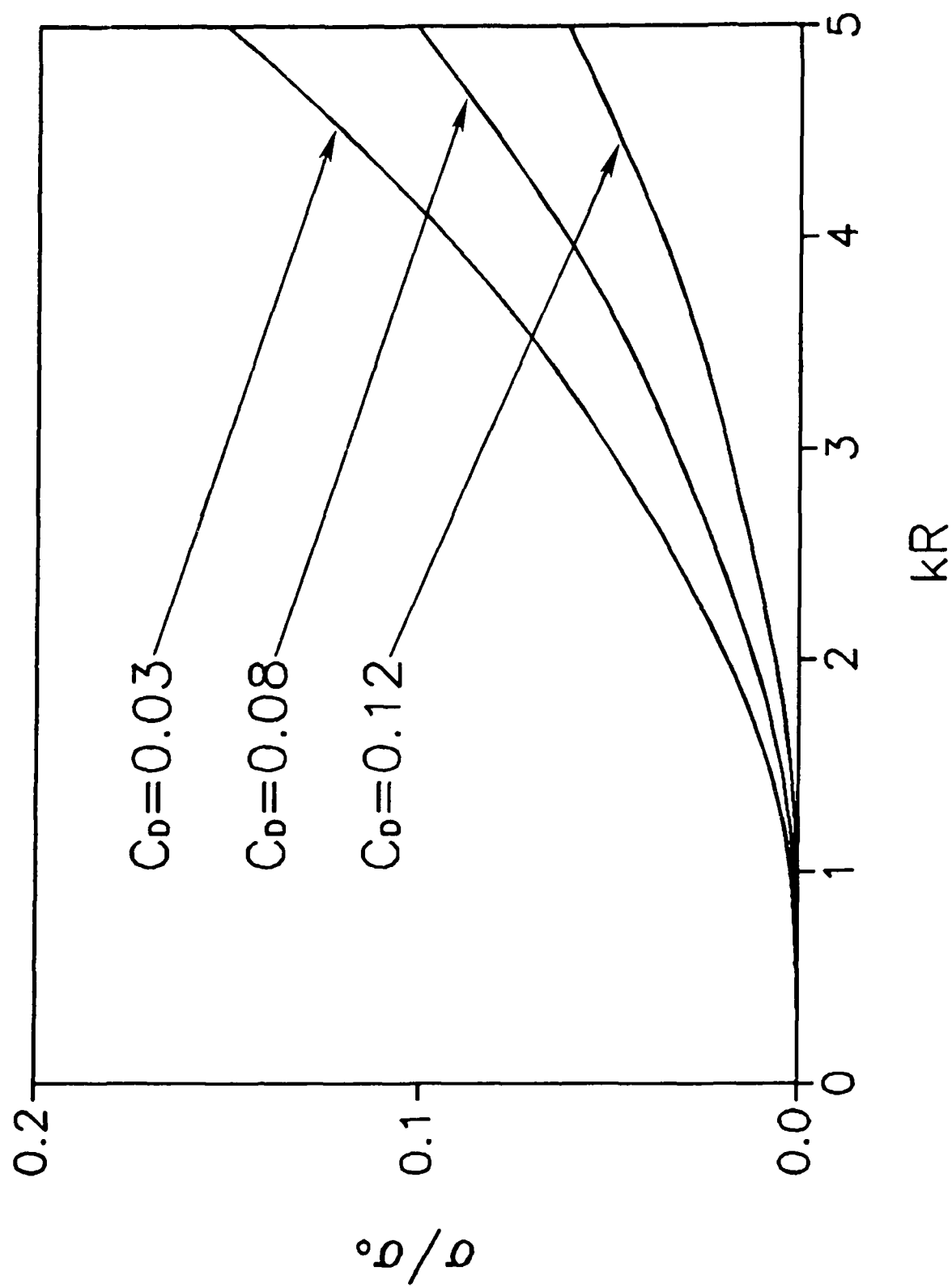
$C_D=0.03$

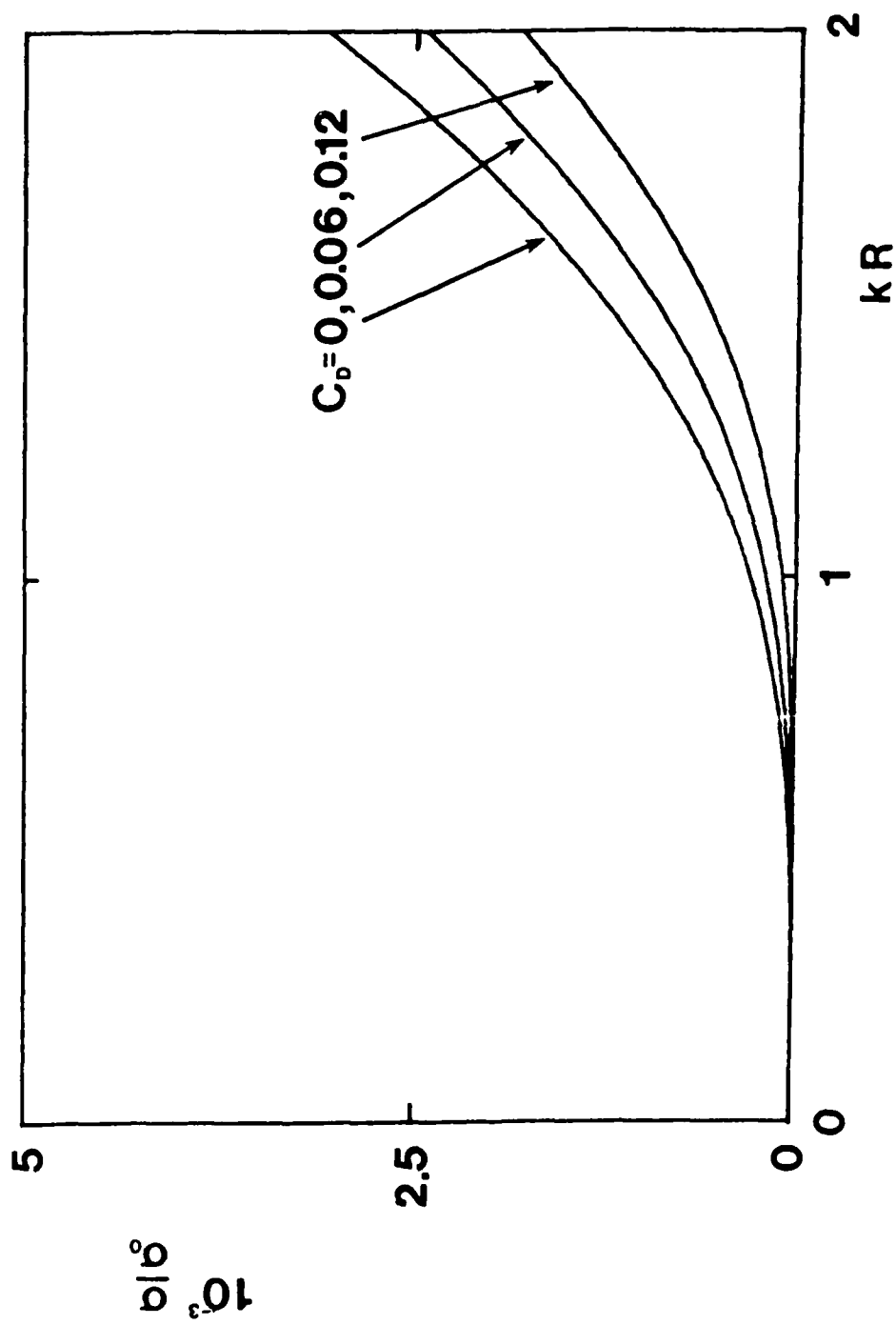$d\sigma/d\Omega\sigma_\circ$

δ (degrees)

100

50

0

0

15

30

Zumer et al.
Fig. 8(b)

Zumer et al.
— Fig. 8(c)

Zumer et al
Fig. 9(a)

$10^3 \, q/q_0$

$C_D = 0, 0.06, 0.12$

kR

Zumer et al.
Fig. 9(b)

σ/σ_o

kR

$C_D = 0$

$C_D = 0.06$

$C_D = 0.12$

$\langle R \rangle = 0.13 \ \mu m$

$\lambda_o = 0.63 \ \mu m$

$\mu = 3.9 \times 10^{-3} \ \mu m^{-1}$

thickness (μm)

Zumer et al.
Fig. 11

randomly oriented droplets

highly oriented droplets

$\langle R \rangle = 0.13$ μm

$\lambda_e = 0.63$ μm

$C_D \sim 0.1$

applied field [V/μm]

σ
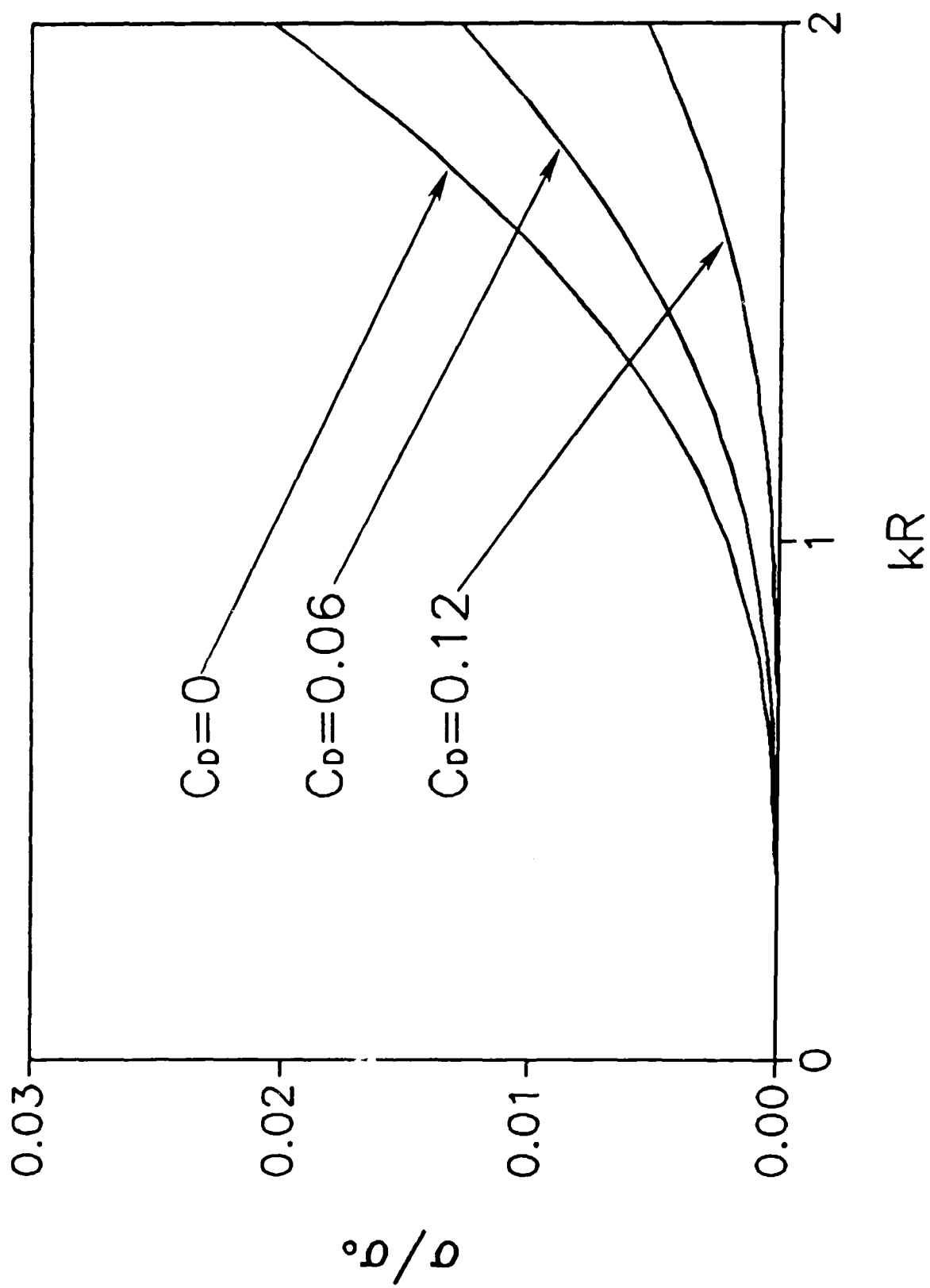$(10^{-4} \times \mu m^2)$

μ
$(10^{-3} \times \mu m^{-1})$

Zumer et al.
Fig. 12
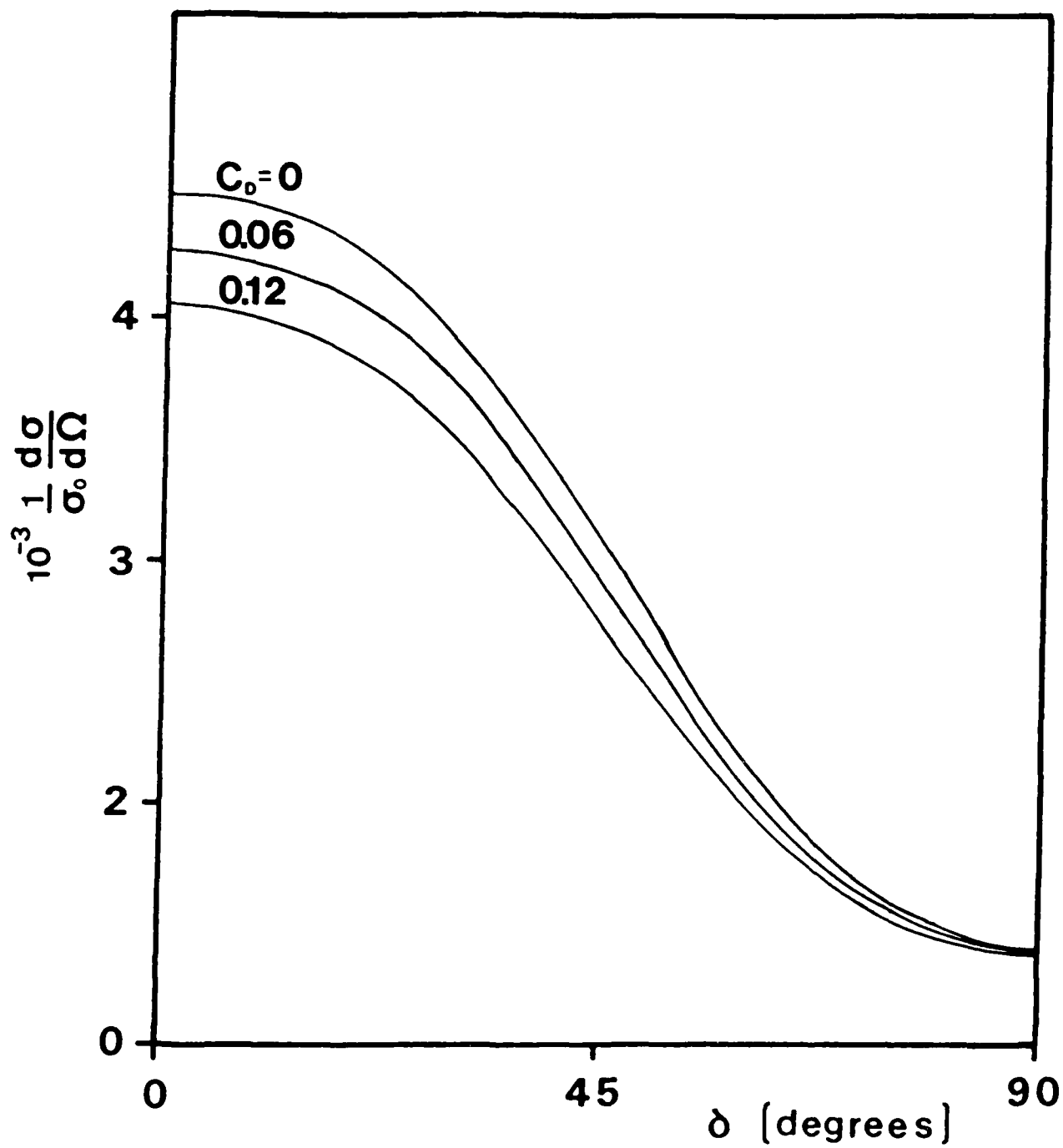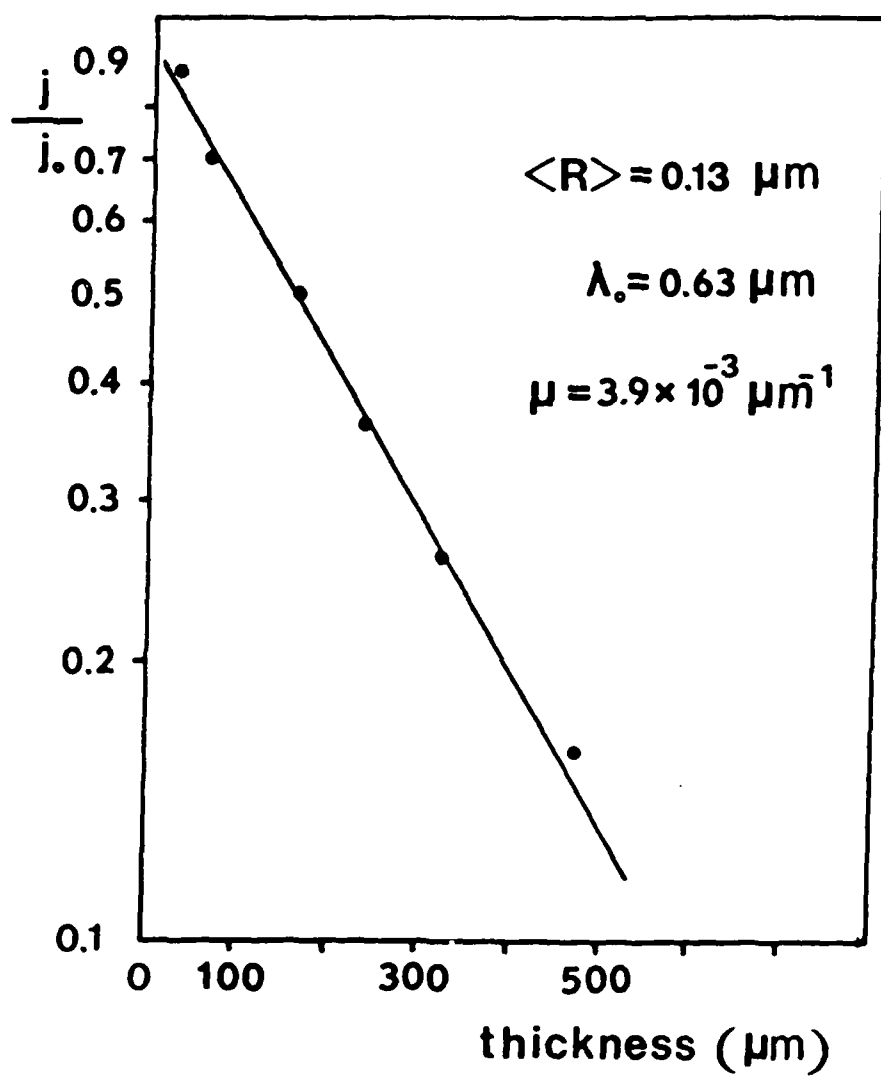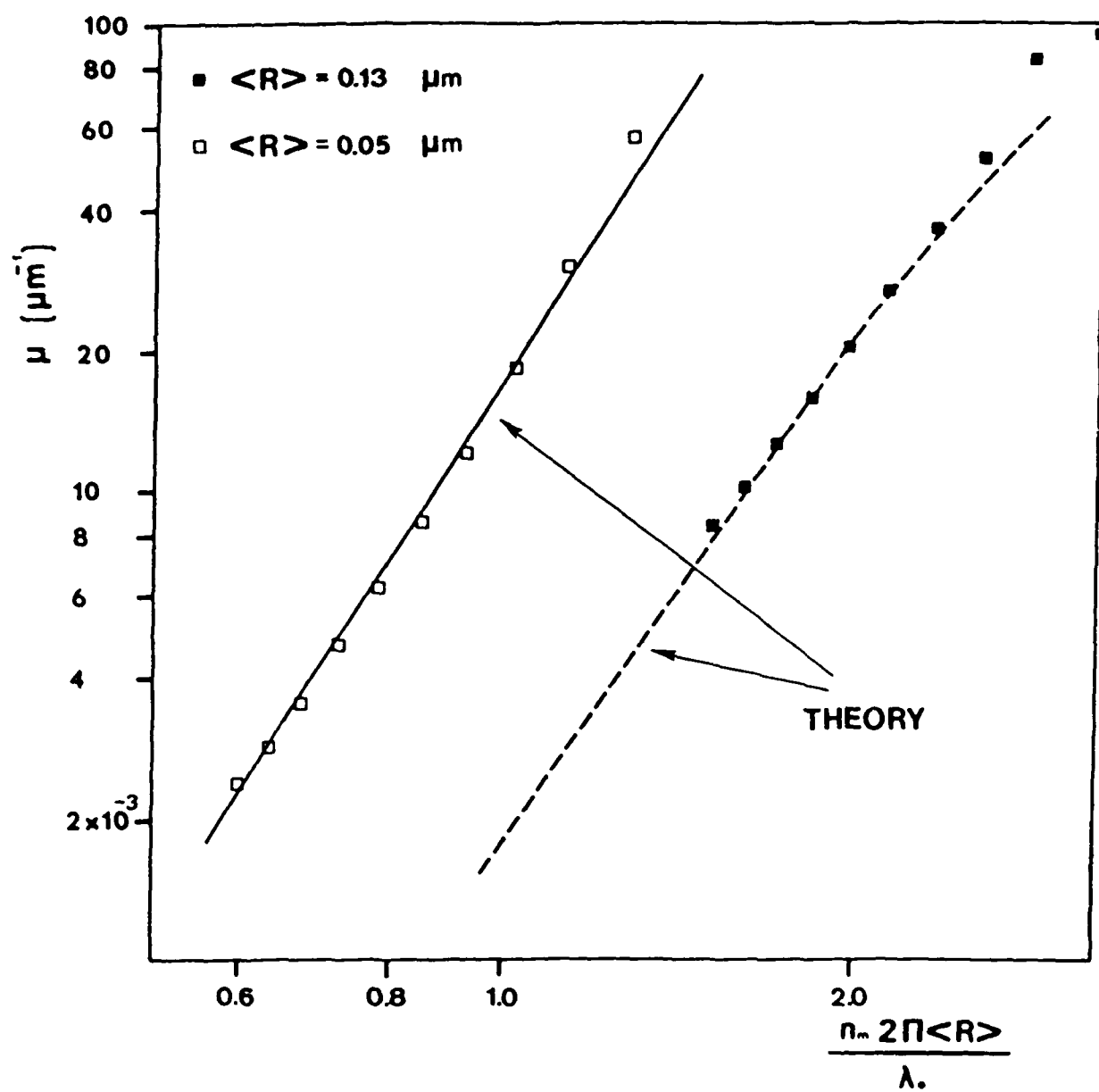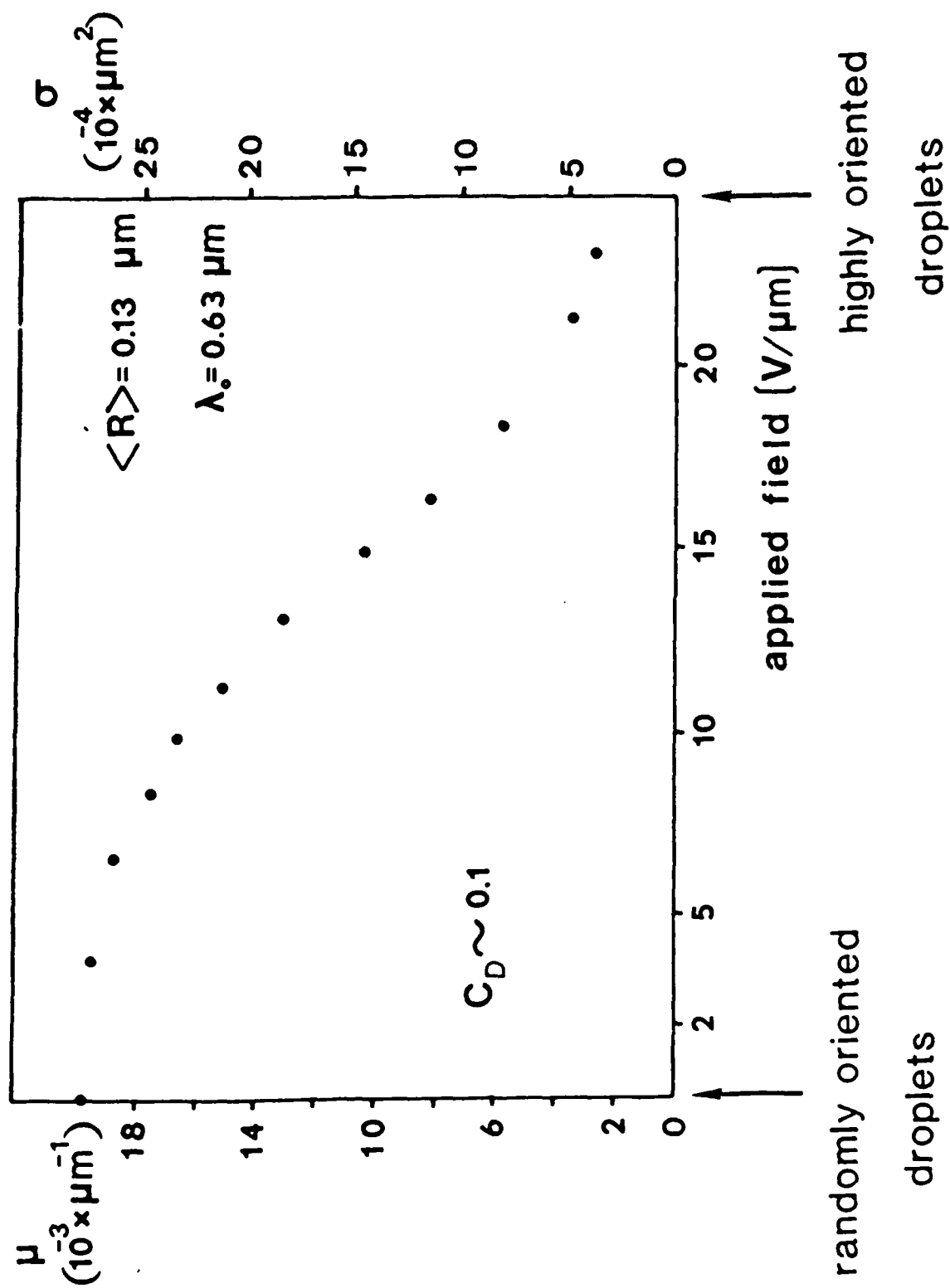
TECHNICAL REPORT DISTRIBUTION LIST, GEN

	No. Copies		No. Copies
Office of Naval Research Attn: Code 1113 800 N. Quincy Street Arlington, Virginia 22217-5000	2	Dr. David Young Code 334 NORDA NSTL, Mississippi 39529	1
Dr. Bernard Douda Naval Weapons Support Center Code 50C Crane, Indiana 47522-5050	1	Naval Weapons Center Attn: Dr. Ron Atkins Chemistry Division China Lake, California 93555	1
Naval Civil Engineering Laboratory Attn: Dr. R. W. Drisko, Code L52 Port Hueneme, California 93401	1	Scientific Advisor Commandant of the Marine Corps Code RD-1 Washington, D.C. 20380	1
Defense Technical Information Center Building 5, Cameron Station Alexandria, Virginia 22314	12 high quality	U.S. Army Research Office Attn: CRD-AA-IP P.O. Box 12211 Research Triangle Park, NC 27709	1
DTNSRDC Attn: Dr. H. Singerman Applied Chemistry Division Annapolis, Maryland 21401	1	Mr. John Boyle Materials Branch Naval Ship Engineering Center Philadelphia, Pennsylvania 19112	1
Dr. William Tolles Superintendent Chemistry Division, Code 6100 Naval Research Laboratory Washington, D.C. 20375-5000	1	Naval Ocean Systems Center Attn: Dr. S. Yamamoto Marine Sciences Division San Diego, California 91232	1